

Effects of the Incorporation of Bioactive Particles on Physical Properties, Bioactivity and Penetration of Resin Enamel Infiltrant

Ana Ferreira Souza¹, Marina Trevelin Souza², Janaína Emanuela Damasceno¹, Paulo Vitor Campos Ferreira³, Gabriela Alves de Cerqueira¹, Flávio Henrique Baggio Aguiar¹, Giselle Maria Marchi¹

¹Department of Restorative Dentistry, Piracicaba Dental School, Campinas State University – UNICAMP, Piracicaba, São Paulo, Brasil; ²Laboratory of Vitreous Materials, Department of Materials Engineering, Federal University of São Carlos, São Carlos, São Paulo, Brasil; ³Department of Restorative Dentistry, Dental Materials Division, Piracicaba Dental School, Campinas State University – UNICAMP, Piracicaba, São Paulo, Brasil

Correspondence: Ana Ferreira Souza, Department of Restorative Dentistry, Piracicaba Dental School, Campinas State University – UNICAMP, Avenida Limeira, 901, Piracicaba, São Paulo, Brasil, 13414-903, Tel +55 098 98191-4015, Fax +55 019 2106-5218, Email fsana.ufma@gmail.com

Purpose: The resinous infiltrant lacks remineralizing activity. This research aimed to develop and evaluate bioactivity, physico-mechanical properties and penetration of resin infiltrants containing Biosilicate or nanohydroxyapatite.

Methods: Experimental resin infiltrant (ERI; 75/25 wt.% TEGDMA/BisEMA) was divided among the groups Pure Experimental (PE); ERI + Biosilicate 5 or 10% (Bio5; Bio10), ERI + 10% nanohydroxyapatite (Hap10), and Icon (DMG, Germany). Bioactivity was analyzed by SEM, EDS and FT-IR/ATR after soaking in SBF. Degree of conversion (DC), sorption and solubility (SO; SOL), flexural strength, modulus of elasticity (FS; E-modulus), contact angle (CA) and penetration were characterized. Extent of penetration was analyzed by treating white spot lesions (WSL) in human dental enamel samples with the infiltrants and subsequently analyzing specimens by confocal laser scanning microscopy. Data from each test were submitted to ANOVA and Tukey's tests ($p < 0.01$).

Results: SEM, EDS and FT-IR showed the formation of precipitates and increase in the rates of Ca and P in the groups with bioactive particles, after storage in SBF. Hap10 showed higher DC and CA values than all the other groups. Groups Bio5 and Bio10 showed CA values similar to those of Icon, higher SO and SOL values, and reduction in other properties. All infiltrants were capable of penetrating into the WSLs.

Conclusion: The incorporation of Biosilicate (5 or 10%) or nanohydroxyapatite (10%) into ERI induced mineral deposition on the surface and did not compromise infiltration and penetration into WSLs, however, compromising their physico-mechanical properties.

Keywords: dental caries, dental enamel, hydroxyapatite, scanning electron microscopy, confocal laser scanning microscopy

Introduction

The resin infiltrant (RI) is indicated for the treatment of early carious lesions – white spot lesions (WSL), in which mineral loss occurs without surface cavitation.¹ RI is a low-viscosity material that fills the porosity of these lesions, restores the integrity of dental tissue without requiring prior wear and obliterates the bacterial acid diffusion pathways, thereby paralyzing progression of the carious lesion.² Resin materials are, however, examples of artificial surfaces heavily colonized by cariogenic biofilms, which is largely due to the absence of a buffer effect.³ This absence has been associated with high rates of occurrence of secondary caries in tissues adjacent to resin restorations.³

The incorporation of compounds, such as bioactive particles that promote a remineralizing effect into resin materials, is a strategy that could help to reduce the occurrence of secondary caries.^{4–7} These so-called bioactive materials are capable of establishing interaction with natural human tissues, and are used with the aim of replacing or complementing the functions of these tissues.^{8,9} In dentistry, several investigations have shown the effectiveness of bioactive particles applied to dental tissue, with benefits related to mineral deposition on the treated surfaces.^{4,5,7,10–13} Hydroxyapatite and Biosilicate are examples of these particles.

Hydroxyapatite particles, especially at the nanoscale, can form a bioactive layer on dental tissues with characteristics very similar to those of natural tissues.¹⁴ In addition to biocompatibility and bioactivity, hydroxyapatite has a morphology and crystalline structure similar to that of natural tooth apatite.^{15,16} Its incorporation into dental materials has previously been investigated, and its remineralizing capacity has been reported.^{4,5,10,17,18} However, limitations have also been reported, especially related to the rheological and mechanical properties of the resulting resin material.^{19,20}

Biosilicate, a bioactive glass ceramic material that has also been investigated for use in several dental applications, has shown that when in contact with fluids, is capable of releasing ions and forming hydroxyapatite crystals on the substrate surface.^{11,21} Studies have reported its ability to promote control of erosion lesions, in addition to preventing demineralization and promoting remineralization of caries lesions.¹¹ Furthermore, a broad spectrum antimicrobial property, including anaerobic bacteria, has been observed for Biosilicate,²² however, up to now no studies investigating its incorporation into dental resin material have been found in the literature.

For hydroxyapatite, some published reports on its incorporation into resin enamel infiltrant were identified,^{4,23} however, they did not analyze the contact angle, flexural strength, surface morphology, or mineral deposition after immersion in simulated body fluid. Considering the positive results relative to the interaction of these particles with dental tissues, especially with dental enamel, their association with a material used in the treatment of WSLs could provide anti-caries properties, thereby optimizing the treatment available at present.

The aim of this study was to evaluate the influence of incorporating bioactive particles of Biosilicate (5 or 10% by weight) or nanohydroxyapatite (10% by weight) into the composition of an experimental resin infiltrant with regard to the properties of bioactivity, degree of conversion (%), sorption and solubility ($\mu\text{g}/\text{mm}^3$), flexural strength (MPa), modulus of elasticity (GPa), contact angle ($^\circ$) and penetration. The null hypotheses tested in this study were: 1) The incorporation of bioactive particles into the resin infiltrant would be unable to induce mineral deposition on the material; 2) The incorporation of bioactive particles would not promote changes in the physical-mechanical properties of the experimental resin infiltrant and 3) the incorporation of bioactive particles would not compromise the penetration of the resin infiltrant into WSLs in dental enamel.

Materials and Methods

Preparation of Infiltrants

The concentrations of bioactive particles used were defined in a pilot study. Experimental resin infiltrates (ERI) were handled in a temperature-controlled environment at 25°C and under yellow light. The monomer base was used in a proportion of 74 wt% triethylene glycol dimethacrylate (TEGDMA), 24.5 wt% ethoxylated bisphenol A dimethacrylate (BisEMA), and the photoinitiator system used was 0.5 wt% camphorquinone (CQ) and 1 wt% ethyl 4-dimethylamino-benzoate (EDAB). This composition represented the Pure Experimental (PE).

The groups with particles were formed by adding either 5 wt% or 10 wt% of Biosilicate (P2O5-Na2O-CaO-SiO2; mean diameter of 5 μm ; LaMaV-UFSCar, São Carlos, SP, Brasil) or 10 wt% of nanohydroxyapatite (Sigma-Aldrich, Steinheim, Germany) to the PE. Resin and particles were mixed for 24 h using a magnetic stirrer at 120 rpm. Two concentrations of Biosilicate were used, because no reports investigating its incorporation in dental resin materials were found in the literature. The commercial control group was represented by the resin infiltrant Icon (IC) (DMG Dental Materials, Hamburg, Germany) (Table 1).

Bioactivity

Analyses were performed using Scanning Electron Microscopy (SEM), Energy Dispersive Spectroscopy (EDS) and Fourier Transform Infrared Spectroscopy/Attenuated Total Reflectance (FT-IR/ATR) to observe the surface morphology and composition, respectively, of the samples without immersion (0 h) and after immersion in SBF for 30 days (30 d).²⁴ A representative sample per group was used for each test. The SBF solution was prepared according to ISO 23317:2014 standards. For each group and for each time (0 h or 30 d) samples of 8 mm in diameter and 2 mm in thickness were made in polyvinylsiloxane molds (Express XT Putty Soft-VPS; 3M ESPE, St. Paul, MN, USA). A polyester strip (Airon; Maquira, Maringá, PR, Brazil) was used to ensure the smoothness of the specimen surfaces. The samples were light-

Table 1 Groups Described by Their Composition According to the Bioactive Particles Used

Group	Composition
Icon	70–95% wt TEGDMA; <2.5% wt CQ and additions*
PE	98.5% wt blend TEGDMA-BisEMA; 0.5% wt CQ; 1% wt EDAB
Bio5	93.5% wt blend TEGDMA-BisEMA; 0.5% wt CQ; 0.9% wt EDAB; 5% wt Biosilicate
Bio10	88.5% wt blend TEGDMA-BisEMA; 0.5% wt CQ; 0.9% wt EDAB; 10% wt Biosilicate
Hap10	88,5% wt blend TEGDMA-BisEMA; 0.5% wt CQ; 0.1% wt EDAB; 10% wt nanohydroxyapatite

Notes: *According to the manufacturer (DMG Dental Materials, Hamburg, Germany). Compounds were purchased from Sigma-Aldrich (Steinheim, Germany).

Abbreviations: PE, Pure Experimental; Bio5, Experimental + 5% Biosilicate; Bio10, Experimental + 10% Biosilicate; Hap10, experimental + 10% nanohydroxyapatite; TEGDMA = triethylene glycol dimethacrylate; BisEMA, ethoxy bisphenol A glycidyl dimethacrylate; CQ, camphorquinone; EDAB, ethyl 4-(dimethylamino) benzoate.

activated with LED light (1000 mW/cm² of irradiance; Valo Corded; Ultradent, South Jordan, UT, USA) for 40s. Samples from 0 h (not stored in SBF) were stored dry in microtubes (Flex-tube; Eppendorf, Hamburg, Germany) in an oven at 37 °C. Samples from 30 days of storage were individually stored in 150 mL of SBF and kept in an oven at 37 °C.²⁴ After 30 days, the samples were stored in microtubes and kept in an oven at 37 °C.

For the SEM analysis, the samples were sputter-coated with gold and analyzed at a working distance of 28 mm, with an accelerating voltage of 15 kV (JSM 5600 PV – JEOL, Tokyo, Japan). For Energy Dispersive Spectroscopy (EDS) analysis, the Vantage Microanalysis System (NORAN Instruments – Middleton, WI, USA) coupled to the SEM was used. The samples were coated with carbon and analyzed at 100x magnification, counting time of 100s, and PHA Deadtime between 20% and 25%. An analysis of 9 distinct areas per representative sample per group was performed to obtain the mean percentage rates by weight of elements Ca and P in each sample. For FT-IR/ATR analysis, after the storage period, all specimens were gently rinsed with water and kept in desiccators with silica gel, at room temperature for slow drying, and submitted to FTIR/ATR (Shimadzu, IRTracer-100, Kyoto, Japan) analysis.

Degree of Conversion

The degree of conversion (DC) values were obtained by recording the methacrylate absorption peak (6165 cm⁻¹) before and after polymerization of the material.²⁵ For each reading (n = 7, DC in %) one drop was inserted into an apparatus created by means of overlapping polished glass microscope slides, creating a space of 0.2 mm. For reading, the set was placed on the support matrix of the Fourier Transform Infrared Spectroscopy apparatus coupled to the ATR (FTIR – Vertex 70, Bruker Optik GmbH, Ettlingen, Germany) and the laser beam was focused on the center of the sample. Analyses were performed using Opus v.6 software (Bruker Optics, Ettlingen, Germany).

The spectrum of the non-polymerized material was obtained, and then light activation was performed with an LED light device (Valo Corded; Ultradent), by placing the device tip in contact with the upper glass slide, perpendicular to the material, for 40s (1000 mW/cm² irradiance). Afterwards, a new reading was performed. The degree of conversion was obtained by dividing the value calculated for the area of spectrum after polymerization by value calculated for the area of the unpolymerized material.

Water Sorption and Solubility

The water sorption and solubility tests were based on ISO 4049:2009 specification, except for specimen dimensions.²³ Eight resin infiltrant disks (n = 10; 5 mm in diameter and 1 mm thick) were made for each group using a polyvinyl siloxane mold (Express XT Putty Soft-VPS; 3M ESPE), and light activated under a polyester strip (Airon; Maquira) for 40s (Valo Corded; Ultradent). All specimens were stored in a desiccator containing silica gel (37 °C) and weighed daily on a precision analytical balance (AUW220D Shimadzu, Kyoto, Japan) until a constant mass (m1) was obtained, with a variation in weight of less than 0.002 mg in 24 hours.

The volume (V) of each disk was calculated using a digital caliper (Mitutoyo, Kanagawa, Japan), and the specimens were stored in microtubes containing 1.5 mL of deionized water at 37 °C for seven days. Then, the specimens were washed in running water for 5s, dried with absorbent paper, and weighed to obtain m2. Afterwards, the specimens were again stored in a desiccator containing silica gel, at 37 °C and were weighed daily until a new constant weight (m3) was obtained. SO was calculated by using the equation: $SO = (m2 - m3)/V$. SOL was calculated using the equation: $SOL = (m1 - m3)/V$.

Flexural Strength and Modulus of Elasticity

Specimens of each group (n = 15) were made in rectangular format, measuring 7 mm in length, 2 mm in width and 1 mm in thickness, using polyvinyl siloxane molds (Express XT Putty Soft-VPS; 3M ESPE).²³ Each material was inserted into the mold and polymerized for 40s, with an LED light source (1000mW/cm² of irradiance; Valo Corded; Ultradent) positioned perpendicular to the material. The specimens were kept in a dry oven at 37°C for 24 h and then underwent a three-point flexural strength (FS) test on the universal testing machine (Instron 4111; Instron Corp., Dayton, OH, USA). A speed of 0.5 mm/min and a load of 50 N was applied. The modulus of elasticity (E-modulus) values was obtained in GPa and the flexural strength in MPa.

Contact Angle

The average contact angle (CA) of the materials was obtained by dispensing drops (n = 8) of infiltrant onto polished glass microscope slides.²⁵ The drops (approximately 1 µL) were dispensed with a syringe positioned perpendicularly to the glass slide, and the images were captured with a camera coupled to the goniometer device (Ramé-hart – 500F1, Succasunna, USA). The measurements of the angles formed between drop and surface were analyzed using drop shape analysis software (DROPimage Advanced; Ramé-hart-500F1, Succasunna, NJ, USA). The mean values of the contact angles on each side of the drop were calculated for each group.

Penetration

The infiltrant penetration into white spot lesions on enamel was analyzed by using the indirect dye marking technique.²⁶ Enamel samples were obtained from healthy extracted human third molars, stored in a 0.1% thymol solution (pH 7) for a period shorter than 3 months. The study was approved by the Research Ethics Committee of the Piracicaba Dental School, under registration CAAE 20224019.1.0000.5418. For this study, the ethics committee waived the application of the consent form, since the teeth used, which were donated by a dental surgeon, were extracted and stored in a single bottle, which made it impossible to identify the patients. The tooth roots were sectioned in a metallographic cutter (Buehler LTD., Lake Bluff, IL, USA). The coronal portion was sectioned in the mesiodistal direction to use the buccal and palatal surfaces of the teeth. Then, a cylindrical diamond drill mounted on a high-speed turbine (KaVo Dental, São Paulo, Brazil) was used to cut samples measuring 4x4x2 mm.

The enamel surfaces were smoothed with 600 and 1200 grit abrasive paper, under irrigation, and polished with felt discs and diamond paste. The specimens were selected according to their mean initial microhardness, obtained by using a microhardness tester (HMV-2000; Shimadzu Corporation, Tokyo, Japan) with a Knoop indenter and a load of 25 g for 10s. Five indentations were performed at 100 µm equidistant from the center of the surface, and specimens with mean hardness between 320 ± 26 were selected. For simulation of initial caries lesions in enamel, the specimens were individually immersed in 10mL of demineralizing solution (17.8mM CaCl₂, 8.8mM KH₂PO₄, 100mM of lactic acid, and 1.0mM NaN₃; pH adjusted to 4.3 using KOH) stored in an oven at 37°C for 10 days.²⁷ The solution was changed daily.

For infiltration of white spot lesions, the surfaces were etched with 15% hydrochloric acid (Icon Etch, DMG, Hamburg, Germany) for 120s, followed by washing with water for 30s. The samples were stored separately in 1 mL of 0.1% rhodamine B isothiocyanate ethanolic solution (RITC, Sigma Aldrich, Steinheim, Germany) for 12 h so that the pores were stained with red fluorophore. After this period, the samples were washed and dried by applying air jets (10s). Icon Dry (99% ethanol) was applied for 30s, followed by application of the infiltrant designated for each group. The infiltrant was applied with a pipette (M25, Microman, Gilson Medical Electronics, France) and remained on the surface for 3 minutes, followed by light activation for 40s (Valo, Ultradent) with an irradiance of 1000 mW/cm². The application

was repeated, allowing the material to remain for 1 minute, as recommended by the manufacturer, again followed by light activation.

Then, ± 1 mm thick slices of infiltrated enamel were obtained by sectioning the specimens with a diamond disk fitted to a metallographic cutter, used perpendicular to the specimen surface. The slices were polished (Arotec S/A Indústria e Comércio) with 2000 granulation water abrasive paper (Sandpaper sheets, Norton) under cooling. Afterwards, the enamel slices were immersed in a 30% hydrogen peroxide solution at 37 °C for 12 hours, to remove excess red fluorophore that had not been incorporated into the infiltrant. After this period, specimens were washed with water for 60s. Two-dimensional images (XY-scan) were obtained using a Confocal Laser Scanning Microscope (Leica, TCS SP8; Leica, Heidelberg, Germany), in fluorescence mode, at 40x magnification, to detect the region filled by the infiltrants, stained with Rhodamine B. Visual analysis of penetration was performed.

Statistical Analysis

Data were analyzed using GraphPad Prism software version 9.0 (GraphPad Software; San Diego, USA). Data show normal distribution (Shapiro–Wilk $p > 0.05$). Comparative analysis was performed with the One-way ANOVA followed by Tukey multiple comparisons tests. The significance level adopted for all analyses was 1% ($\alpha < 0.01$).

Results

Bioactivity

From the semi-quantitative analysis of EDS, an increase in the rates of percentage by weight of Ca and P was observed in all groups containing bioactive particles after 30 days of soaking in SBF. For ERI samples containing 5% Biosilicate (Bio5), an increase in Ca (1.77x) and P (56x) rates were observed after soaking in SBF for 30 days (Figure 1). At 0 h, the mean rates of each element were 5.12% Ca and 0.09% P, and 9.08% Ca and 5.06% P after 30 days. The group containing 10% Biosilicate (Bio10) also showed a significant increase in the rates of Ca (4.65x) and P (60x) after 30 days of soaking in SBF. The mean rates of each element at 0h were 5.76% of Ca and 0.18% of P, while after 30 days of immersion, 26.8% of Ca and 10.85% of P were observed.

The group containing 10% nanohydroxyapatite (Hap10) showed the highest rates of Ca and P at both time intervals and showed an increase in mean rates after 30 days of soaking. A mean increase of 1.35x in Ca and 1.61x for P was observed. At 0 h, the mean rates of each element for this group were 26.71% for Ca and 8.53% for P, while after 30 days

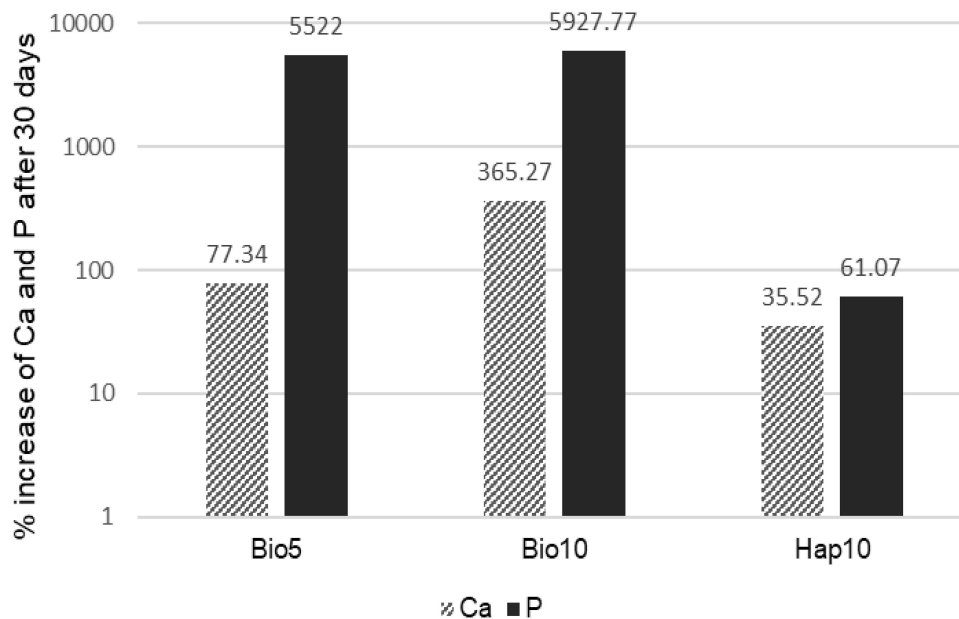


Figure 1 Comparative graph of the increase in percentage rates by weight of Ca and P of the groups containing bioactive particles at 0 h and after 30 days of storage in SBF.

of storage, rates of 36.2% of Ca and 13.74% of P were observed. **Figure 1** shows the percentages of increase in Ca and P rates of groups containing bioactive particles at 0 h and after 30 days of storage in SBF.

The SEM analysis allowed us to observe the difference between the groups without bioactive particles (IC and PE), which showed similar surfaces at 0 h and after 30 days (**Figure 2**), without formation of precipitates, while the groups containing particles showed intense growth of spherical agglomerates and precipitates on the surface after soaking in SBF.

In images at higher magnification (x1000) of the ERI without soaking and after 30 days of soaking in SBF solution (**Figure 3**), it is possible to observe the high density of a crystalline phase covering the surface.

Analysis by FT-IR/ATR

After 30 days of SBF immersion (**Figure 4b**), the presence of hydroxycarbonate apatite (HCA) was detected in the groups containing bioactive particles in their composition, which was not observed for the groups without particles. This can be explained by the mineral precipitation resulting from the interaction of the particles with the SBF solution. For the groups

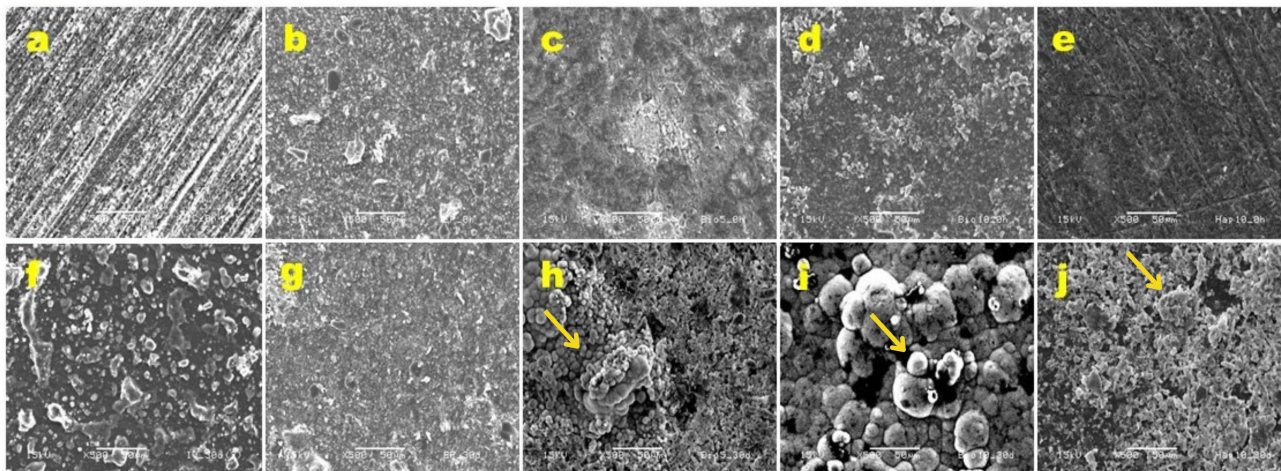


Figure 2 SEM micrographs of infiltrant samples without storage (0 h; upper row) and after 30 days of storage in SBF (30 d; lower row). 500x magnification. Size bar: 50 μ m. (a) IC 0 h, (b) PE 0 h, (c) Bio5 0 h, (d) Bio10 0 h and (e) Hap10 0 h; (f) IC 30 d, (g) PE 30 d, (h) Bio5 30 d, (i) Bio10 30 d and (j) Hap10 30 d. Yellow arrows: spherical agglomerates/precipitates.

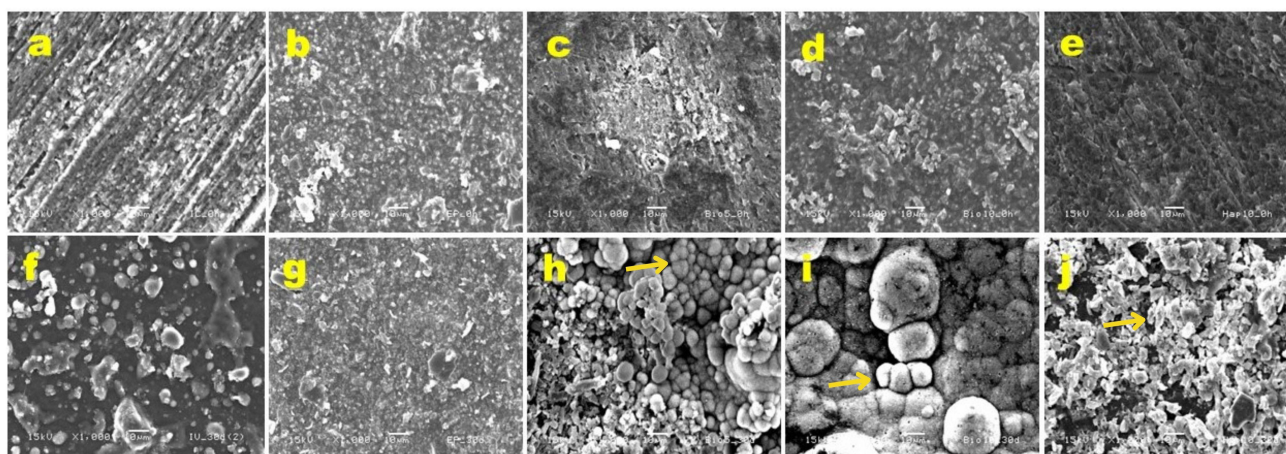


Figure 3 SEM micrographs of infiltrant samples without storage (0 h; upper row) and after 30 days of storage in SBF (30 d; lower row). 1000x magnification. Size bar: 10 μ m. (a) IC 0 h, (b) PE 0 h, (c) Bio5 0 h, (d) Bio10 0 h and (e) Hap10 0 h; (f) IC 30 d, (g) PE 30 d, (h) Bio5 30 d, (i) Bio10 30 d and (j) Hap10 30 d. Yellow arrows: spherical agglomerates/precipitates.

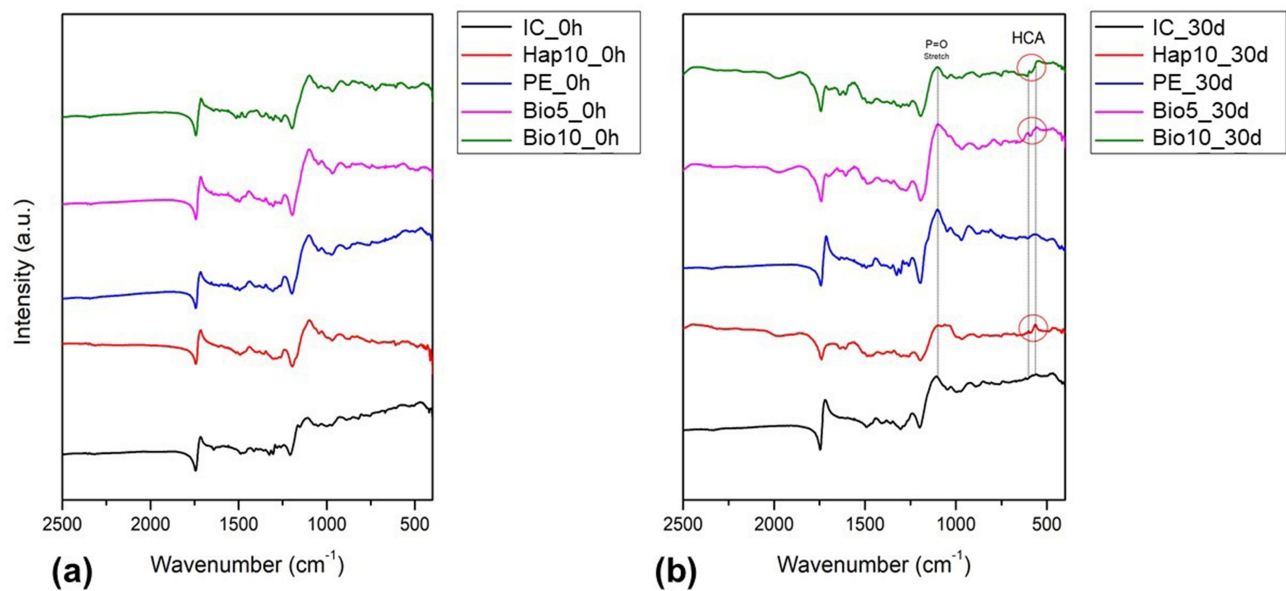


Figure 4 FT-IR/ATR spectrum of infiltrant specimens without immersion (0h – a) and after immersion (30d – b) in SBF.

without immersion (Figure 4a), HCA was not detected in any of the groups, which may have occurred due to the trapping of the particles in the organic matrix.

For the physical-mechanical properties tested, the mean and standard deviation values for each group are shown in Table 2.

Degree of Conversion

The Hap10 Group was observed to have statistically higher values than the other study groups ($P < 0.0001$). The groups with the lowest degree of conversion were Bio5 and Bio10.

Sorption and Solubility

The IC Group had statistically lower sorption values than all the other groups ($P < 0.0001$). Furthermore, the PE group was observed to have statistically lower values than the Hap10 Group. Hap10 did not differ from Bio5 and Bio10 ($P > 0.01$). PE, Bio5, and Bio10 did not differ from each other ($P > 0.01$). For solubility, the groups with the addition of Biosilicate had statistically higher values than the other groups ($P < 0.0001$). The PE Group showed the lowest values and did not differ only from IC. In addition, Bio10 group was observed to be the one with the statistically highest values in the study, differing even from the Bio5 Group.

Table 2 Mean and Standard Deviation (sd) of Degree of Conversion (%), Sorption ($\mu\text{g}/\text{mm}^3$), Solubility ($\mu\text{g}/\text{mm}^3$), Flexural Strength (MPa), E-Modulus (GPa), and Contact Angle ($^\circ$) by Group

Variable	Infiltrant					p value
	Icon	PE	Bio5	Bio10	Hap10	
Degree of conversion (%)	46.1 (3.54) C	81.5 (0.49) B	27.1 (3.04) D	24.1 (2.85) D	88.9 (0.40) A	<0.001
Sorption ($\mu\text{g}/\text{mm}^3$)	58.2 (2.76) C	111 (4.39) B	123 (10.5) AB	117 (11.1) AB	130 (3.71) A	<0.001
Solubility ($\mu\text{g}/\text{mm}^3$)	2.71 (0.88) D	0.51 (0.39) D	25.5 (4.56) B	30.7 (3.33) A	5.28 (1.66) C	<0.001
Flexural Strength (MPa)	103 (17) A	46.3 (8.39) B	27.4 (6.35) C	29.2 (8.93) C	47 (5.38) B	<0.001
E-modulus (GPa)	1.63 (0.16) A	0.46 (0.05) B	0.23 (0.06) C	0.22 (0.05) C	0.51 (0.06) B	<0.001
Contact Angle ($^\circ$)	23.2 (0.97) B	24.4 (0.57) B	23.9 (1.40) B	24.9 (0.67) B	31.4 (3.10) A	<0.001

Note: Different letters indicate statistical difference between columns.

Flexural Strength and Modulus of Elasticity

For both flexural strength and modulus of elasticity, IC showed statistically higher values than the other groups ($P < 0.0001$). Furthermore, Groups PE and Hap10 did not differ from each other and had higher values than Groups Bio5 and Bio10 ($P < 0.001$). The groups with Biosilicate did not differ from each other.

Contact Angle

For contact angle, the Hap10 Group had statistically higher values when compared with the other study groups ($P < 0.0001$). The other study groups showed no significant differences among them.

Penetration

Figure 5 shows micrographs, obtained by confocal laser scanning microscopy in the fluorescence mode, of the interfaces between resin infiltrant and dental enamel for each material applied. Extensions of resin infiltrants in dental enamel were observed for all groups tested. For the groups with bioactive particles incorporated into them, gaps were observed at the infiltrant-dental enamel interface.

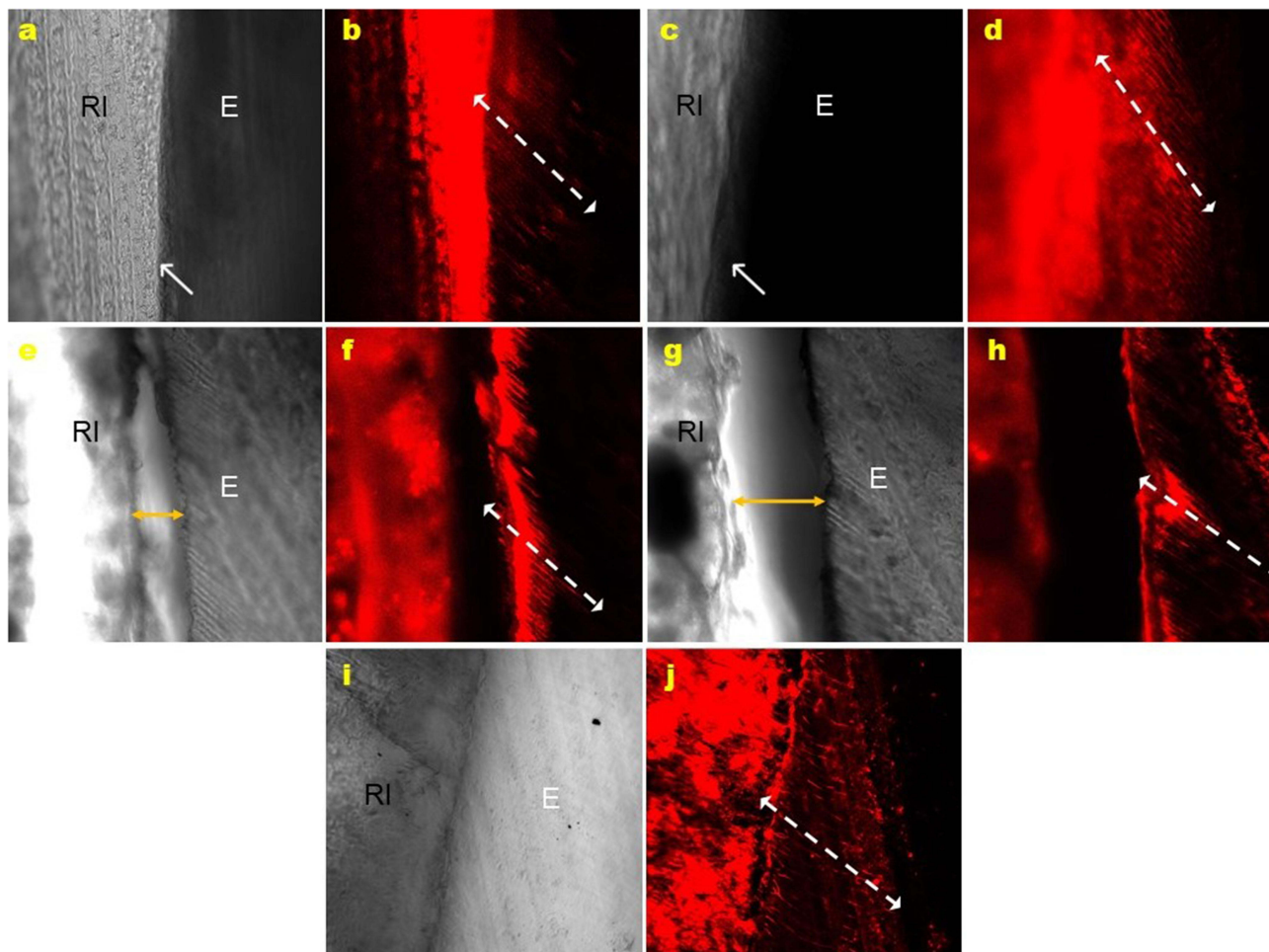


Figure 5 Micrographs obtained by confocal laser scanning microscopy in fluorescence mode, for analysis of the resin infiltrant penetration. (a and b) Icon (IC); (c and d) PE; (e and f) Bio5; (g and h) Bio10; (i and j) Hap10.

Abbreviations: RI, resinous infiltrant; E, enamel; White arrow, infiltrant-enamel interface; White dashed arrow, extension of the infiltrant within the WSL; Yellow arrow, infiltrant-enamel gap.

Discussion

The present study analyzed the influence of the incorporation of Biosilicate or nanohydroxyapatite into experimental resin infiltrants, on their bioactivity, physical-mechanical properties, and penetration into substrates. Two null hypotheses tested were rejected, because (1) an increase in the rates of Ca and P was observed in the samples of infiltrants containing bioactive particles after storage in simulated body fluid (SBF) and (2) the incorporation of bioactive particles into resin infiltrant promoted statistically significant changes in all the properties tested ($p < 0.01$). The third null hypothesis was not rejected, as (3) the penetration of infiltrants containing bioactive particles, into early enamel caries lesions, was not impaired.

One of the assays that could help us to predict a material's bioactivity *in vivo* is the one that uses SBF solution and analyzes the formation of apatite on its surface.²⁸ A study has reported that when bioglass bioactive particles come into contact with oral fluids, apatite hydroxycarbonate forms on their surfaces, with mineral precipitation because of the release of ions such as Si^{4+} , OH^- , Na^+ , Ca^{2+} and PO_4^{3-} .¹³ In this study, the incorporation of bioactive particles into the resin infiltrant was capable of increasing the Ca and P concentration on the surface of the materials after soaking in SBF. Amid supersaturation of Ca^{2+} and PO_4^{3-} ions, they can diffuse into carious lesions in the dental enamel, favoring the formation of apatite and increasing its mineral content.^{4,5,7} Through micro-ct analysis, it was observed that the application of infiltrant containing 5 or 10% of nanohydroxyapatite was able to increase the mineral density of initial caries lesions in enamel.²⁹

The presence of bioactive particles in resin material has also been reported to be capable of promoting the neutralization of acid by products, raising the pH of the surrounding microenvironment to above 5.5, which is the critical pH for mineral dissolution of dental tissue.²⁰ This property of ionic release added to the resin material could then help prevent secondary caries lesions, by making the enamel surrounding the infiltrated area less predisposed to chemical dissolution resulting from caries activity.

The physical-mechanical properties of resin materials are highly dependent on the quality of the three-dimensional polymeric network formed after polymerization.³⁰ The degree of conversion (DC), which corresponds to the consumption of aliphatic double bonds during monomeric polymerization, has a great influence on the final properties of the resin material.³⁰ The Hap10 group had a significantly higher DC when compared with all the other groups. These results corroborated the findings of previous studies,^{4,5,23} which also observed a significant increase in the degree of conversion of infiltrants or composite resins containing 10% hydroxyapatite. This could be related to the size of particles in nanometric range that were incorporated. The incorporation of particles on a smaller scale has been reported to allow greater light transmission through the resin material.³¹ Another factor that may be related is the high crystallinity of the particles and their effect on light diffraction and scattering, which may have optimized the polymerization.^{4,5}

The groups into which Biosilicate was incorporated showed significantly reduced degree of conversion rates. The Biosilicate particles used had micrometric dimensions, with an average size of $5\mu\text{m}$. The lower values when compared with the Hap10 group were assumed to possibly being due to the larger particle size, which impaired light transmission.³¹ Another possibility could have been a difference in crystallinity between the particles and incompatibility between the refractive indices of the particles and the resin matrix, which may have caused greater scattering and lower light transmission.^{4,5} The non-silanization of particles has also been related to lower light transmission due to the formation of gaps at the resin-particle interface during polymerization.³² The high percentage of unreacted monomers, indicated under polymerization of the network, compromised the mechanical properties of the material, making it more susceptible to degradation.³⁰

The highest water sorption rates were observed for the groups containing bioactive particles and for the PE group. Resin materials undergo inherent hydrolytic degradation, which accelerates this process, reducing their physical-mechanical properties and, consequently, their longevity.³⁰ For groups containing particles, this increase in sorption could be attributed to the increased hydrophilicity of the composites due to their addition.^{20,33}

Another related factor may be the lower quality of the polymeric network formed in the presence of non-silanized particles. The addition of particles also resulted in increased solubility, which may be related to the dissolution of the particles in the aqueous medium, as previously reported for resin-based materials containing bioactive particles,^{5,19,20} and

the detachment of particles from the matrix due to non-silanization. This chemical degradation was related to oxidation and hydrolysis processes, which occurred in the presence of water.³⁴ A trend towards an increase in the hydrophilicity of resin matrix materials was observed as the rate of bioactive particles incorporated increased.^{5,20}

The groups containing Biosilicate had the highest solubility rates. Solubility corresponds to the leaching of components from the material volume; therefore, according to the results of the present study, it could be inferred that the lower degree of conversion presented by the groups containing Biosilicate may also have contributed to its high solubility. The high rate of unreacted monomers may have resulted in an impaired polymer network, favoring water infiltration between the chains, leaching of unreacted monomers, and greater contact with bioactive particles, allowing ionic release. The opposite was true for the Hap10 group, which had higher degree of conversion and significantly lower solubility than that shown by Groups Bio5 and Bio10. However, degradation is necessary for there to be bioactivity. As these particles degrade, silicon, calcium, sodium ions and phosphate groups are released to the physiological environment, thus dissolving themselves so that the HCA layer formation can occur.³⁵ So, for bioglass to be bioactive, the presence of water is a key factor that starts the cascade reaction that transforms it into a bioactive agent,¹³ therefore, there must be a flow of water in the material.

The lower sorption and solubility rates of the Icon Group and the lower solubility of the PE Group reinforced the more hydrophobic nature and the higher quality of the polymeric network formed when compared with groups containing bioactive particles. PE had a lower mean solubility values than the commercial Icon Group, corroborating the findings of previous studies.^{23,36} This may have been due to the presence of BisEMA in the composition, which resulted in a higher degree of conversion of the material.³⁰

For flexural strength and modulus of elasticity, the experimental groups had significantly lower mean values when compared with Icon. The particles were incorporated into the resin matrix without prior silanization, to avoid interfering with the release of specific ions, such as Ca, PO, and Si, responsible for promoting the remineralization of dental hard tissues. The results of the present study corroborated those of previous investigations that also observed that the particle non-silanization could result in a weak bond between particles and resin matrix.^{5,20} This could reduce the transfer of stress between these two phases, directly impacting the flexural strength of the materials.^{5,20} It is possible to assume that the incorporation of the non-silanized particles into the resin matrix resulted in a highly flexible and high free volume polymeric network, due to the gaps that formed at the interface between resin matrix and particles during polymerization.³⁰

The highest mean modulus of elasticity values, after Icon (IC), was observed for the PE and Hap10 groups, which showed no statistical difference between them. The absence of particles in the PE group and the better distribution of nanoparticles within the resin matrix in the Hap10 group may have favored this result.³³ It has been reported that the larger interfacial surface area provided by nanoparticles could increase the transfer of load between the matrix and particles.³³

As regards the contact angle (CA), Hap10 showed the highest values, differing statistically from all the others. This may have been due to particle size (<200nm), which at the nanoscale, had a greater influence on the increase in resin material viscosity.^{37,38} Even when incorporated in equal amounts by weight, nanoparticles resulted in a higher degree of matrix thickening, due to the significantly larger total surface area when compared with microparticles, as well as the resulting larger volume of particles.³⁷ In a previous investigation, it was observed that the incorporation of filler particles into resin infiltrate, to a lesser extent, reduced infiltrant penetration in early caries lesions,³⁹ due to the increase in the amount of organic matrix necessary for coating the particles, which would reduce the rate of availability of organic matrix, leading to a reduction in fluidity of the material.^{38,39} In the present study, however, this higher level of CA shown by Group Hap10 did not compromise its penetration into enamel caries lesions. This result corroborates the findings of Elembaby et al²⁹ who incorporated 5 and 10% nanohap in resin infiltrant and observed penetration in initial enamel caries lesions comparable to the Icon control group. For groups containing Biosilicate, the smaller volume of microparticles incorporated into the ERI, when compared with the volume of nanoparticles, may have resulted in higher rates of free resin matrix, thus not harming the contact angle of the materials.^{33,39} For Groups Icon and PE, the lower mean contact angle values may have been due to the absence of particles and predominance of TEGDMA monomer in Icon, which has a low molecular weight.^{30,40}

All infiltrants demonstrated the ability to penetrate into enamel caries lesions. The analysis by Confocal Laser Scanning Microscopy allowed us to observe a similar pattern of extension of the resin infiltrates between the Icon commercial control and the experimental groups, as was also observed previously.²⁹ Therefore, the incorporation of particles did not harm penetration. Infiltrants containing particles, however, exhibited displacement of the surface layer of material from the infiltrated-dental enamel interface. This may have been due to the reduction in the mechanical properties of the resulting polymer associated with displacements resulting from the procedures of preparing samples for analysis. Thin slices (≈ 1 mm) were prepared by sectioning with a diamond disc fitted to a metallographic cutter, which may have generated intense stress at the interface. However, it is noteworthy that use of the infiltration technique does not advocate the creation of a thick layer of resin material on the enamel surface, but rather its penetration into the demineralized pores, which was observed for all groups.

Relative to the properties of solubility and contact angle, Group PE showed a behavior similar to that of the commercial Icon control, with no statistical difference. Furthermore, it also exhibited significantly higher DC. It could be inferred that the composition of infiltrants proposed in this study had the potential to be investigated in future applications. In general, incorporation of bioactive particles into the resin infiltrant impacted on the physical-mechanical properties, especially for the groups into which Biosilicate was incorporated. This was largely due to the non-silanization of these particles, which affected the quality of the polymer network formed. However, the mechanism of action of the resin infiltrant is based on the penetration of this material into the carious lesions; therefore, since the degree of penetration was satisfactory, these properties may not affect the effectiveness of the treatment.

A limitation of this study is the fact that the bioactivity was not tested by simulating the dynamics that occur in the oral cavity. Future studies can analyze the mineral deposition and surface morphology of infiltrants under conditions of salivary flow and brushing, for example.

Conclusion

The incorporation of the bioactive particles investigated at the proposed concentrations was able to promote the formation of Ca and P precipitates on the surface of the resin infiltrants and did not harm their penetration into the WSLs. However, the incorporation compromises the physical-mechanical properties of the resinous infiltrant, especially for groups containing Biosilicate.

Ethics Approval

The study was approved by the Research Ethics Committee of the Piracicaba Dental School, under registration CAAE 20224019.1.0000.5418.

Acknowledgments

We thank Prof. Dr. Vandilson Pinheiro Rodrigues (Federal University of Maranhão) for his assistance in the statistical analyses. We would also like to thank Professors Dr. Roberto Ruggiero Braga and Dr. Bruna Fronza for their help in performing the degree of conversion test.

Author Contributions

All authors made a significant contribution to the work reported, whether that is in the conception, study design, execution, acquisition of data, analysis and interpretation, or in all these areas; took part in drafting, revising or critically reviewing the article; gave final approval of the version to be published; have agreed on the journal to which the article has been submitted; and agree to be accountable for all aspects of the work.

Funding

This study was supported by grants from CAPES (Coordenação de Aperfeiçoamento de Pessoal de Nível Superior; #88887.342761/2019-00) and FAPESP (Fundação de Amparo à Pesquisa do Estado de São Paulo; #2019/11850-1 and 2019/25093-8).

Disclosure

Miss Ana Ferreira Souza reports grants from FAPESP (Fundação de Amparo à Pesquisa do Estado de São Paulo) and CAPES (Coordenação de Aperfeiçoamento de Pessoal de Nível Superior), outside the submitted work. The authors declare that they have no other conflicts of interest in this work.

References

- Kielbassa AM, Muller J, Gernhardt CR. Closing the gap between oral hygiene and minimally invasive dentistry: a review on the resin infiltration technique of incipient (proximal) enamel lesions. *Quintessence Int.* 2009;40(8):663–681.
- Paris S, Meyer-Lueckel H, Kielbassa AM. Resin infiltration of natural caries lesions. *J Dent Res.* 2007;86(7):662–666. doi:10.1177/154405910708600715
- Nedeljkovic I, De Munck J, Slomka V, Van Meerbeek B, Teughels W, Van Landuyt KL. Lack of buffering by composites promotes shift to more cariogenic bacteria. *J Dent Res.* 2016;95(8):875–881. doi:10.1177/0022034516647677
- Andrade Neto DM, Carvalho EV, Rodrigues EA, et al. Novel hydroxyapatite nanorods improve anti-caries efficacy of enamel infiltrants. *Dent Mater.* 2016;32(6):784–793. doi:10.1016/j.dental.2016.03.026
- Jardim RN, Rocha AA, Rossi AM, et al. Fabrication and characterization of remineralizing dental composites containing hydroxyapatite nanoparticles. *J Mech Behav Biomed Mater.* 2020;109:103817. doi:10.1016/j.jmbm.2020.103817
- Memarpour M, Shafiei F, Rafiee A, Soltani M, Dashti MH. Effect of hydroxyapatite nanoparticles on enamel remineralization and estimation of fissure sealant bond strength to remineralized tooth surfaces: an in vitro study. *BMC Oral Health.* 2019;19(1):1–13. doi:10.1186/s12903-019-0785-6
- Yang SY, Kwon JS, Kim KN, Kim KM. Enamel surface with pit and fissure sealant containing 45S5 bioactive glass. *J Dent Res.* 2016;95(5):550–557. doi:10.1177/0022034515626116
- Hench LL, Splinter RJ, Allen WC, Greenlee TK. Bonding mechanisms at the interface of ceramic prosthetic materials. *J Biomed Mater Res.* 1971;5(6):117–141. doi:10.1002/jbm.820050611
- Vallittu PK, Boccaccini AR, Hupa L, Watts DC. Bioactive dental materials—do they exist and what does bioactivity mean? *Dent Mater.* 2018;34(5):693–694. doi:10.1016/j.dental.2018.03.001
- Alhamed M, Almalki F, Alsalami A, Alotaibi T, Elkatehy W. Effect of different remineralizing agents on the initial carious lesions – a comparative study. *Saudi Dent J.* 2020;32(8):390–395. doi:10.1016/j.sdentj.2019.11.001
- Chinelatti MA, Tirapelli C, Corona SAM, et al. Effect of a bioactive glass ceramic on the control of enamel and dentin erosion lesions. *Braz Dent J.* 2017;28(4):489–497. doi:10.1590/0103-6440201601524
- Pintado-Palomino K, Tirapelli C. The effect of home-use and in-office bleaching treatments combined with experimental desensitizing agents on enamel and dentin. *Eur J Dent.* 2015;09(01):066–73. doi:10.4103/1305-7456.149645
- Tirapelli C, Panzeri H, Lara EHG, Soares RG, Peitl O, Zanutto ED. The effect of a novel crystallised bioactive glass-ceramic powder on dentine hypersensitivity: a long-term clinical study. *J Oral Rehabil.* 2011;38(4):253–262. doi:10.1111/j.1365-2842.2010.02157.x
- Cochrane NJ, Cai F, Huq NL, Burrow MF, Reynolds EC. Critical review in oral biology & medicine: new approaches to enhanced remineralization of tooth enamel. *J Dent Res.* 2010;89(11):1187–1197. doi:10.1177/0022034510376046
- Hannig M, Hannig C. Nanomaterials in preventive dentistry. *Nat Nanotechnol.* 2010;5(8):565–569. doi:10.1038/nnano.2010.83
- Yamagishi K, Onuma K, Suzuki T, et al. A synthetic enamel for rapid tooth repair. *Nature.* 2005;433(7028):819. doi:10.1038/433819a
- Bossù M, Saccucci M, Salucci A, et al. Enamel remineralization and repair results of Biomimetic Hydroxyapatite toothpaste on deciduous teeth: an effective option to fluoride toothpaste. *J Nanobiotechnology.* 2019;17(1):1–13. doi:10.1186/s12951-019-0454-6
- Scribante A, Dermenaki Farahani MR, Marino G, et al. Biomimetic Effect of Nano-Hydroxyapatite in Demineralized Enamel before Orthodontic Bonding of Brackets and Attachments: visual, Adhesion Strength, and Hardness in in Vitro Tests. *Biomed Res Int.* 2020;2020:1–9. doi:10.1155/2020/6747498
- Chen L, Xu C, Wang Y, Shi J, Yu Q, Li H. BisGMA/TEGDMA dental nanocomposites containing glyoxylic acid-modified high-aspect ratio hydroxyapatite nanofibers with enhanced dispersion. *Biomed Mater.* 2012;7(4):045014. doi:10.1088/1748-6041/7/4/045014
- Yang SY, Piao YZ, Kim SM, Lee YK, Kim KN, Kim KM. Acid neutralizing, mechanical and physical properties of pit and fissure sealants containing melt-derived 45S5 bioactive glass. *Dent Mater.* 2013;29(12):1228–1235. doi:10.1016/j.dental.2013.09.007
- Ubal dini ALM, Pascotto RC, Sato F, Soares VO, Zanutto ED, Baesso ML. Effects of bioactive agents on dentin mineralization kinetics after dentin bleaching. *Oper Dent.* 2020;45(3):286–296. doi:10.2341/18-272-L
- Martins CHG, Carvalho TC, Souza MGM, et al. Assessment of antimicrobial effect of Biosilicate[®] against anaerobic, microaerophilic and facultative anaerobic microorganisms. *J Mater Sci Mater Med.* 2011;22(6):1439–1446. doi:10.1007/s10856-011-4330-7
- Sfalcin RA, Correr AB, Morbidelli LR, et al. Influence of bioactive particles on the chemical-mechanical properties of experimental enamel resin infiltrants. *Clin Oral Investig.* 2017;21(6):2143–2151. doi:10.1007/s00784-016-2005-y
- Carvalho EM, Ferreira PVC, Gutiérrez MF, et al. Development and characterization of self-etching adhesives doped with 45S5 and niobophosphate bioactive glasses: physicochemical, mechanical, bioactivity and interface properties. *Dent Mater.* 2021;37(6):1030–1045. doi:10.1016/j.dental.2021.03.004
- Mathias C, Gomes RS, Dressano D, Braga RR, Aguiar FHB, Marchi GM. Effect of diphenyliodonium hexafluorophosphate salt on experimental infiltrants containing different diluents. *Odontology.* 2019;107(2):202–208. doi:10.1007/s10266-018-0391-0
- Meyer-Lueckel H, Paris S. Infiltration of natural caries lesions with experimental resins differing in penetration coefficients and ethanol addition. *Caries Res.* 2010;44(4):408–414. doi:10.1159/000318223
- Margolis HC, Zhang YR, Lee CY, Kent RL, Moreno EC. Kinetics of enamel demineralization in vitro. *J Dent Res.* 1999;78(7):1326–1335. doi:10.1177/00220345990780070701
- Kokubo T, Takadama H. How useful is SBF in predicting in vivo bone bioactivity? *Biomaterials.* 2006;27(15):2907–2915. doi:10.1016/j.biomaterials.2006.01.017
- Elembaby A, AlHumaid J, El Tantawi M, Akhtar S. The impact of nano-hydroxyapatite resin infiltrant on enamel remineralization: an in vitro study. *Int J Periodontics Restorative Dent.* 2022;42(2):e43–e50. doi:10.11607/prd.5599

30. Fonseca ASQS, Labruna Moreira AD, De albuquerque PPAC, de Menezes LR, Pfeifer CS, Schneider LFJ. Effect of monomer type on the C[dbnd]C degree of conversion, water sorption and solubility, and color stability of model dental composites. *Dent Mater.* 2017;33(4):394–401. doi:10.1016/j.dental.2017.01.010
31. Fujita K, Ikemi T, Nishiyama N. Effects of particle size of silica filler on polymerization conversion in a light-curing resin composite. *Dent Mater.* 2011;27(11):1079–1085. doi:10.1016/j.dental.2011.07.010
32. Feng L, Suh BI, Shortall AC. Formation of gaps at the filler-resin interface induced by polymerization contraction stress. Gaps at the interface. *Dent Mater.* 2010;26(8):719–729. doi:10.1016/j.dental.2010.03.004
33. Misra SK, Mohn D, Brunner TJ, et al. Comparison of nanoscale and microscale bioactive glass on the properties of P(3HB)/Bioglass® composites. *Biomaterials.* 2008;29(12):1750–1761. doi:10.1016/j.biomaterials.2007.12.040
34. Ferracane JL. Hygroscopic and hydrolytic effects in dental polymer networks. *Dent Mater.* 2006;22(3):211–222. doi:10.1016/j.dental.2005.05.005
35. Hench LL. Third-generation biomedical materials. *Science.* 2002;295(5557):1014–1017. doi:10.1126/science.1067404
36. Inagaki LT, Dainezi VB, Alonso RCB, et al. Evaluation of sorption/solubility, softening, flexural strength and elastic modulus of experimental resin blends with chlorhexidine. *J Dent.* 2016;49:40–45. doi:10.1016/j.jdent.2016.04.006
37. Bastos NA, Bitencourt SB, Martins EA, De Souza GM. Review of nano-technology applications in resin-based restorative materials. *J Esthet Restor Dent.* 2020;2020:1–16.
38. Beun S, Bailly C, Dabin A, Vreven J, Devaux J, Leloup G. Rheological properties of experimental Bis-GMA/TEGDMA flowable resin composites with various macrofiller/microfiller ratio. *Dent Mater.* 2009;25(2):198–205. doi:10.1016/j.dental.2008.06.001
39. Askar H, Lausch J, Dörfer CE, Meyer-Lueckel H, Paris S. Penetration of micro-filled infiltrant resins into artificial caries lesions. *J Dent.* 2015;43(7):832–838. doi:10.1016/j.jdent.2015.03.002
40. Sideridou I, Tserki V, Papanastasiou G. Effect of chemical structure on degree of conversion in light-cured dimethacrylate-based dental resins. *Biomaterials.* 2002;23(8):1819–1829. doi:10.1016/S0142-9612(01)00308-8

Clinical, Cosmetic and Investigational Dentistry

Dovepress

Publish your work in this journal

Clinical, Cosmetic and Investigational Dentistry is an international, peer-reviewed, open access, online journal focusing on the latest clinical and experimental research in dentistry with specific emphasis on cosmetic interventions. Innovative developments in dental materials, techniques and devices that improve outcomes and patient satisfaction and preference will be highlighted. The manuscript management system is completely online and includes a very quick and fair peer-review system, which is all easy to use. Visit <http://www.dovepress.com/testimonials.php> to read real quotes from published authors.

Submit your manuscript here: <https://www.dovepress.com/clinical-cosmetic-and-investigational-dentistry-journal>